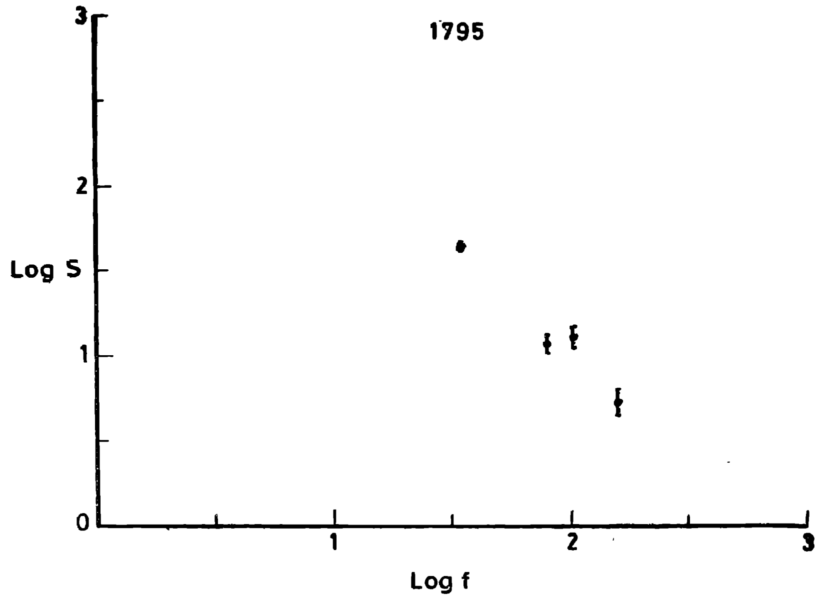

Figure 1j.

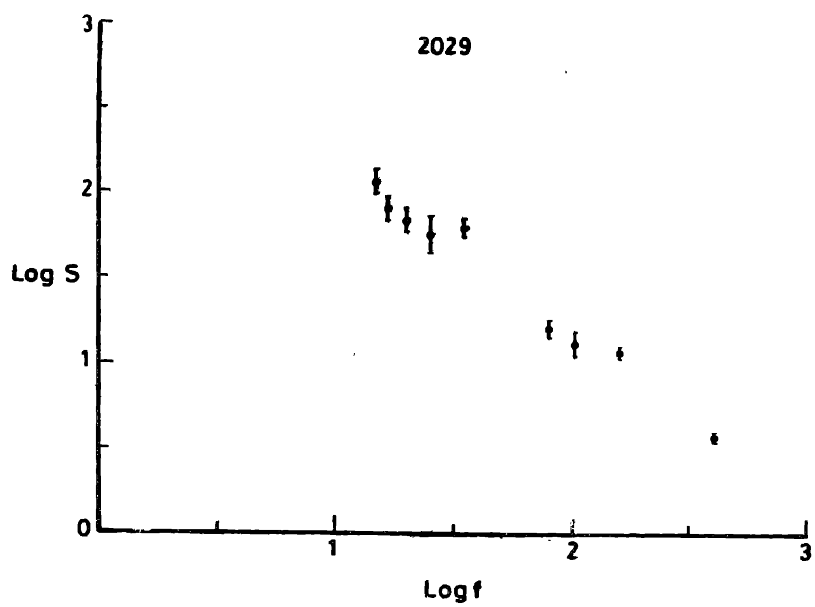

Figure 1k.

steepen. In this model one would expect to observe a critical frequency above which the spectrum steepens, and below which the spectrum is the original one. Measurements of Slee *et al.* (1982) at 80 MHz and 160 MHz revealed that the average spectral index of sources within 0.1 radius of the cluster centre is steep (-0.93 ± 0.03) compated to the mean spectral index of a field sample of radio galaxies (-0.81 ± 0.02). The present results confirm this trend down to decametric wavelenghts.

The detection of diffuse halo type radio emission from clusters of galaxies is important for determining the physical parameters of intracluster gas parameters.

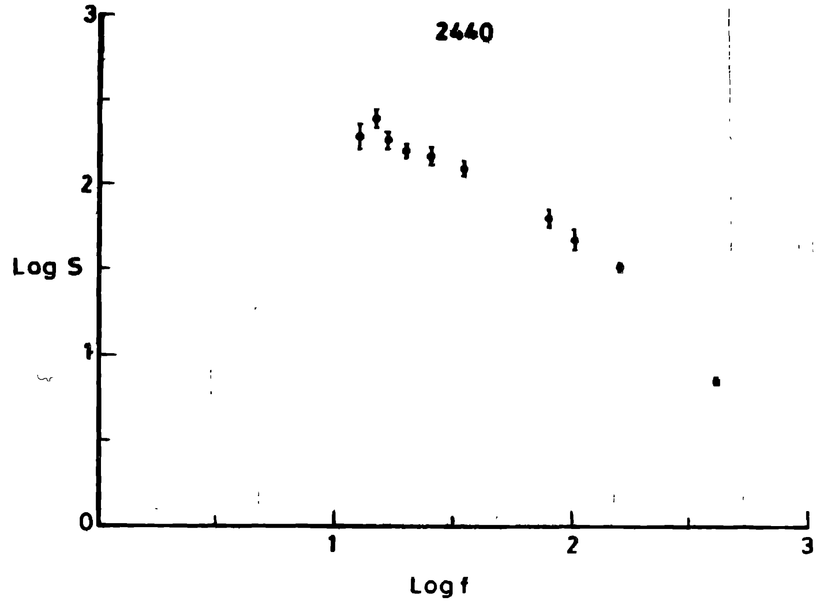

Figure 1l.

Figures 1a to 1l. Plot of log of flux density S vs log of frequency f for various cluster sources.

The Coma cluster is the only source for which there is definite evidence for the existence of a halo from x-rays to decametric radio waves, with a radio spectral index of -1.3 ± 0.2 (see e.g. Sastry & Shevgaonkar 1983). Observations of Hanisch (1980) at 430 MHz and Gavazzi (1978) at 1415 MHz showed the possibility of the existence of a diffuse halo in the cluster A1367. Cane *et al.* (1981) detected an excess in the observed flux at 80 MHz over the expected flux for this source indicating the existence of halo although the excess is not much larger than the uncertainty in their measurements. From the spectrum of A1367 shown in figure 1*h* it is clear that there is no excess flux at any decametric wavelength and the observations do not support the hypothesis of the existence of a halo-type source in the cluster.

Acknowledgements

We thank Messrs Aswathappa, Nanje Gowda and Rajasekhara for their help in the observations.

References

Baldwin, J. E. & Scott, P. F. (1973) *M.N.R.A.S.* **165**, 259.
Braude, S. Ya., Miroshnitschenko, A. P., Sokolov, K. P. & Sharykin, N. K. (1980) *Ap. Sp. Sci.* **76**, 279.
Cane, H. V., Erickson, W. C., Hanisch, R. J. & Turner, P. J. (1981) *M.N.R.A.S.* **409**, 106.
Dagkesamansky, R. D., Gubanov, A. D. & Slee, O. B. (1982) *M.N.R.A.S.* **200**, 971.
Gavazzi, G. (1978) *Astr. Ap.* **69**, 355.
Hanisch, R. J. (1980) *Astr. J.* **85**, 1565.

Joshi, M. N., Kapahi, V. K. & Bagchi, J. (1986) *NRAO workshop on radio continuum processes in clusters of galaxies*, Green Bank.
Kuhr, H., Witzel, A., Pauliny-Toth, I.I.K. & Nauber, U. (1981) *Astr. Ap. Suppl.* **45**, 367.
Sastry, Ch. V. & Shevgaonkar, R. K. (1983) *J. Ap. Astr.* **4**, 47.
Slee, O. B. & Quinn, P. J. (1979) *Proc. Astr. Soc. Aust.* **3**, 332.
Slee, O. B., Wilson, I. R. G. & Siegman, B. C. (1983) *Aust. J. Phys.* **36**, 101.

Bull. Astr. Soc. India (1988) **16**, 192–199

A rapid scan Fourier transform infrared spectrometer

S. K. Jain[1] and M. J. Smyth[2]
[1]*Indian Institute of Astrophysics, Bangalore 560 034*
[2]*Department of Astronomy, Royal Observatory, Edinburgh EH9 3HJ, UK*

Received 1988 June 30; accepted 1988 August 30

Abstract. A rapid scan Fourier transform spectrometer for astronomical infrared spectroscopy, tested at the Cassegrain focus of the 102 cm telescope at Kavalur, is described. The design of the fore-optics and the performance of the spectrometer are discussed.

Key words : Fourier transform spectrometer—spectroscopy

1. Introduction

In the visible domain of the spectrum, the signal-to-noise ratio (SNR) of spectroscopic observations is limited principally by photon noise. In the infrared domain however SNR can be limited by detector noise. It was shown by Fellgett (1951) that in the circumstances of detector-noise-limited measurement a considerable gain in SNR can be achieved if a large number of spectral elements are observed simultaneously; this is the multiplex advantage ('Fellgett's advantage'). Ridgway & Brault (1984) have investigated the range of source brightness, telescope size, and wavelength in which the multiplex advantage holds.

The multiplex advantage is realized practically in the Fourier transform spectrometer (FTS). (e.g. Sakai 1977). Briefly, in a dispersive (e.g., diffraction grating) spectrometer, each spectral element is measured sequentially, whereas in the FTS all the spectral elements are measured simultaneously in Fourier space, and the spectrum is recovered by inverse Fourier transformation of the signal (interferogram). As pointed out by Jacquinot (1954), the optical throughput of interferometric spectrometers is intrinsically higher than that of their dispersive counterparts. This Jacquinot advantage is important for the spectrometry of extended objects, such as nebulae and galaxies, but is also relevant to the seeing-enlarged images of stars when high spectral resolution is required. The availability of infrared detector arrays will reduce the scope of the multiplex advantage relating to a single detector, but nevertheless the number of array elements cannot easily rival the number of spectral elements that can be multiplexed by FTS, and in any case the throughput advantage remains.

An FTS for infrared spectroscopy of astronomical objects has been tested at the Cassegrain focus of the 102 cm telescope at Kavalur. The design of the fore-optics, the characteristics of the interferometer, and the performance of the system are now described.

2. The instrument

The spectrometer comprises the following basic elements: fore-optics, interferometer, control electronics, detector, and data-acquisition and reduction system.

Fore-optics. The optical interface utilizes the interferometer in 'four-port' mode, i.e., making use of the two inputs and two outputs of a Michelson interferometer. If the 'star + sky' signal enters one input, while 'sky' alone enters the other, then the interferogram measured at each output corresponds to the difference of the two inputs; thus first-order subtraction of sky background, a major requirement of measurement in the infrared domain, is performed automatically. Figure 1 shows the fore-optics, similar to a design by Ridgway & Capps (1974). A dichroic filter (not shown) between the aperture plate and the telescope transmits the infrared and reflects the visible component of the light for use in guiding. The two beams, after being deflected into a horizontal plane by two small flats, are collimated by two identical spherical mirrors in a configuration resembling that of a Czerny-Turner spectrograph. The collimated beams enter the interferometer 2° off-axis; returning from the interferometer they again encounter the spherical mirrors which now re-image the focal plane onto the detectors.

The diameter of each spherical mirror is 10 cm and the radius of curvature 100 cm. The corresponding size of the initially f/13 beam is 38.5 mm, and implies, at the maximum interferometer resolving power of 20,000, a field-of-view of nearly 160 arcsec on the sky.

A retractable chopper wheel mounted on a small motor is provided to assist preliminary alignment of the spectrometer.

Interferometer. The instrument is a commercial (Block Engineering Inc.) Michelson inteferometer of classical design, with plane mirrors. A schematic layout of the interferometer is shown in figure 2. It comprises a main interferometer for the astronomical signal and a small auxiliary 'piggy-back' interferometer that generates white-light and monochromatic reference signals. The moving mirror is mounted in an air-bearing, and is translated by an electro-mechanical transducer similar to a loudspeaker coil. The mirror movement is controlled by a constant-velocity servo. The auxiliary interferometer has two detectors which look at, respectively, a laser and a white light source. The white light signal, a sharply peaked interferogram, is used to identify the position of zero path difference and initialize the control unit and data acquisition system. This feature makes it possible to co-add a large number of interferograms coherently in order to increase the SNR. The interferogram from the He-Ne laser (632.8 nm) is used to generate the velocity servo error signal and to provide timing information for sampling the source signal from the main interferometer.

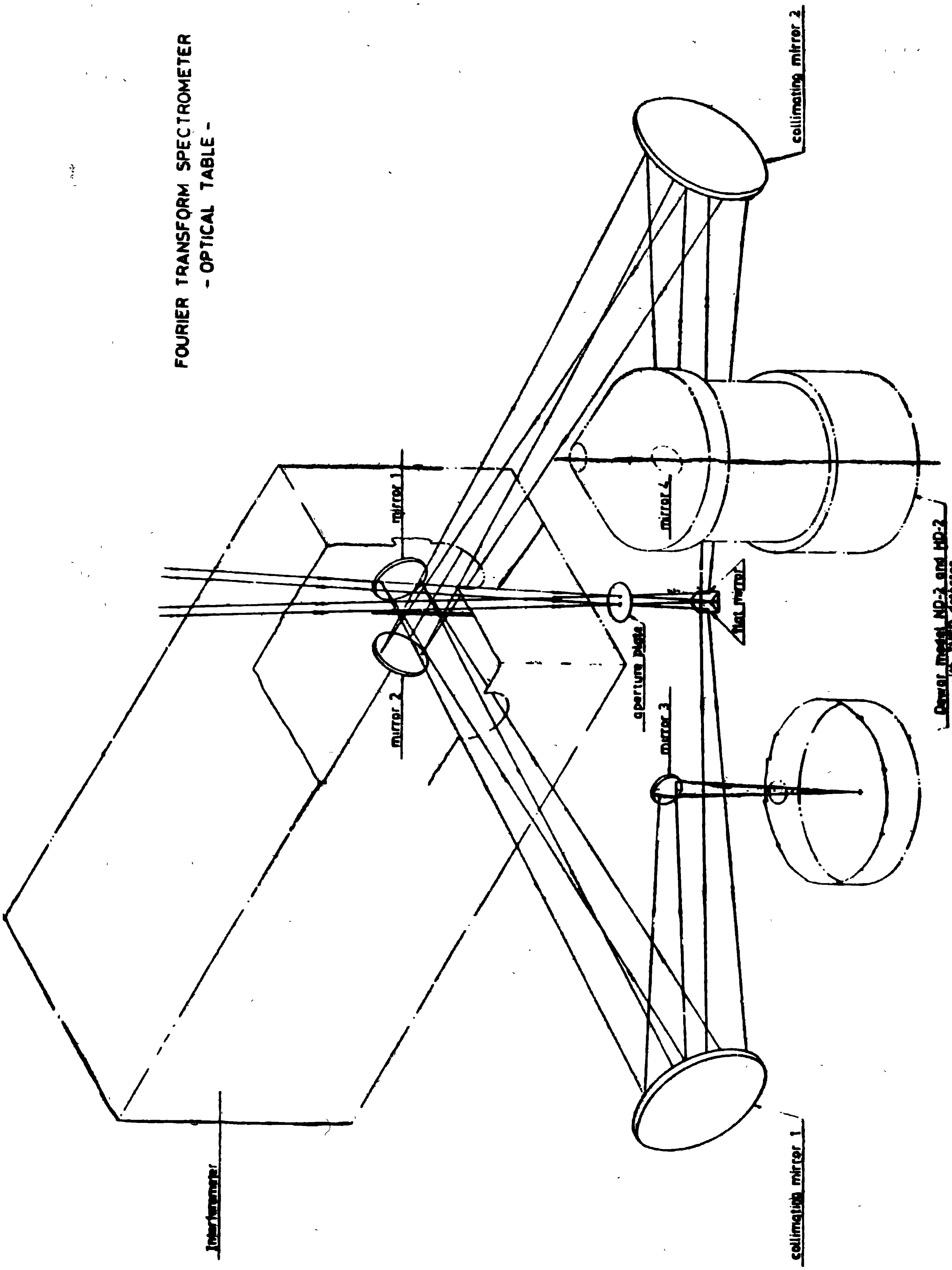

Figure 1. Schematic lay-out of the fore-optics.

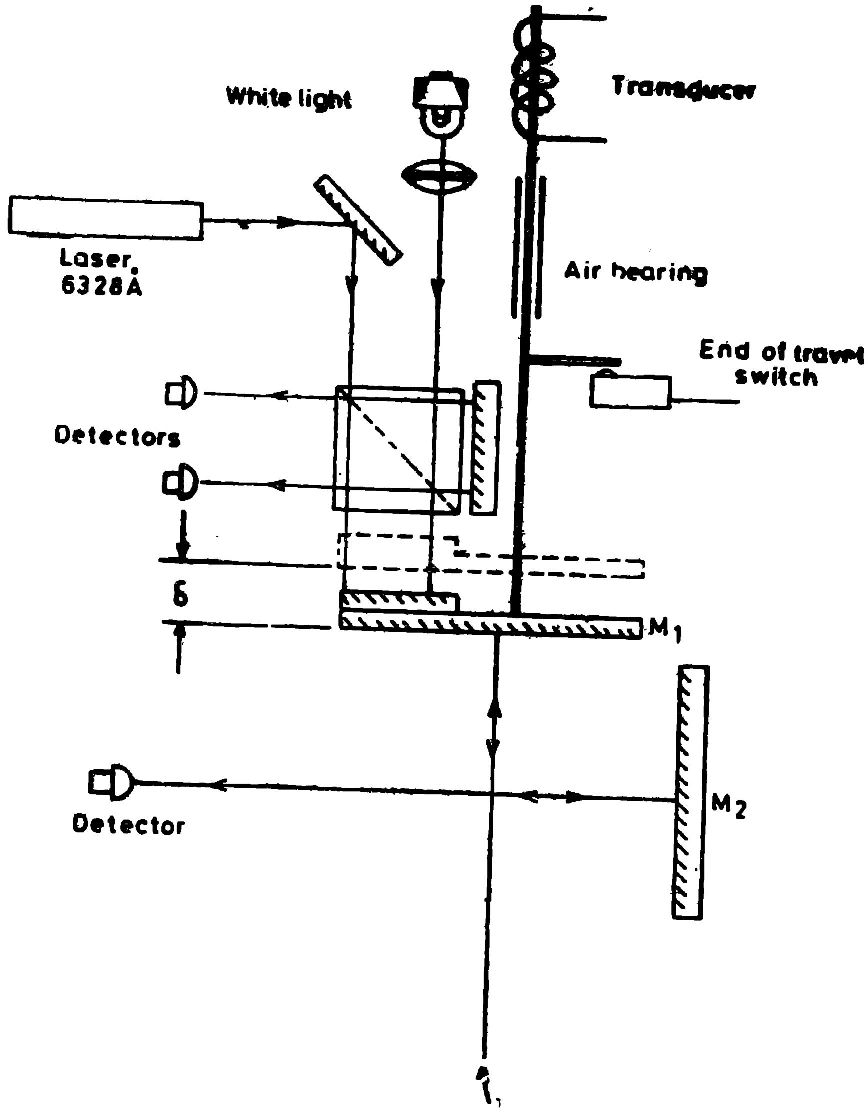

Figure 2. Optical lay-out of the interferometer; B, beam splitter; M1 and M2, flat mirrors

Control electronics. The interferometer is controlled by a unit which houses most of the power supplies, generates signals required by the interferometer drive, and analogue-to-digital converts the main interferogram for the data-processing stage. The sequence of control signals is shown in figure 3.

The monochromatic (laser) reference signal goes to a comparator that detects the zero crossings and generates a square wave. A digital frequency doubler generates a train of pulses whose average area is proportional to the frequency of the monochromatic interferogram and provides velocity information for the servo loop. The velocity is servoed at 2000 laser fringes per second.

The white light interferogram goes to a peak detector which determines the point of zero retardation for the auxiliary interferometer. A SYNC pulse is generated and a train of CLOCK pulses, whose period can be selected to be 1/2,

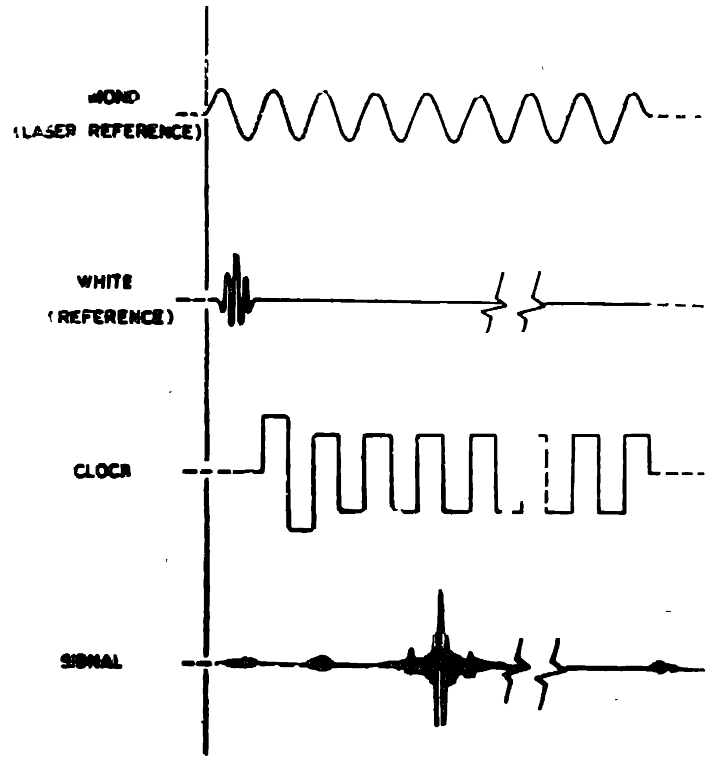

Figure 3. Interferometer signals and their time relationship.

1, 2, 4, 8, or 16 times the period of the mono-chromatic interferogram, is gated ON. It is gated OFF at a predetermined count representing the end of the active scan, and reverse drive is applied, causing the mirror to fly back for the start of another scan.

The auxiliary interferometer is adjusted so that its point of zero retardation comes about 100 fringes before that of the main interferometer. Thus the main interferogram contains samples starting about 100 fringes before zero path difference (ZPD), and these are used in the process of phase correction which will be considered later.

The principal characteristics of the interferometer are given in table 1.

Table 1. Important specifications of the interferometer

Spectral range	0.64–2.5 μm	1–5 μm
Beam splitter	Fe_2O_3	Fe_2O_3
Beam splitter substrate	Quartz	CaF_2
Optical retardations	0.0625, 0.125, 0.25, 0.5, 1.0, 2.0 cm	
Corresponding resolutions	16, 8, 4, 2, 1, 0.5 cm^{-1}	
No. of samples (at 1λ)	1K, 2K, 4K, 8K, 16K, 32K	
Wavenumber precision	0.1 cm^{-1}	
Sampling precision	< 100 A°	
Scan velocity	1.27 mm s^{-1} (CLOCK 2 KHz)	
Velocity precision	Better than 5%	
Sampling interval	632.8 nm × 1/2, 1, 2, 4	
Aperture stop area	> 20 cm^2	
Air pressure required	Between 30 and 55 PSI	

Detector. The detector is a single InSb element of 0.5 mm diameter, mounted in a liquid nitrogen cryostat. The cryostat also houses cold filters, apertures, Fabry lens, pre-amplifier, and CaF_2 window. All these are maintained at liquid nitrogen temperature to minimize thermal background noise. Specifications of the detector element and other components are given in table 2.

Table 2. Detection system specifications

Detector material	Photovoltaic Indium Antimonide (InSb)
Detector size	0.5 mm diameter
NEP	1×10^{-16} $WHz^{-1/2}$
Feedack resistors (77K)	$6.5 \times 10^{8}\Omega$ (LO)
	$7.5 \times 10^{9}\Omega$ (HI)
Filters	1.1–1.7μm, 'K', 'L', three open holes
Apertures	2 mm, 1.5 mm, 1 mm, 0.5 mm, blank

Data acquisition and reduction system. The data are processed in a UNICORN microcomputer linked to the interferometer control unit. The interferogram first passes through a bandpass electronic filter (Krone-Hite) which removes signal frequencies that do not pertain to the occupied spectral range, thus reducing the possibility of intermodulation noise. The resulting signal is 12-bit analogue-to-digital converted and is stored in the memory of the microcomputer. To permit co-adding of up to 4096 (2^{12}) interferograms, the data are stored as 3-byte integers. 4K interferograms, occupying 12K of the computer's main memory, are thus the largest that could be stored internally. Therefore an external 128K static RAM unit has been constructed, operating through the computer's 1 MHz bus. A fast Fourier transform (FFT) program in ROM allows rapid transformation of up to 4K interferogram samples, and either the interferogram or the transformed spectrum can be displayed on the screen or dumped to a dot-matrix printer. This is a very useful facility for rapid checking of the quality of the observations. Interferograms larger than 4K are transferred as binary data files to the VAX 11/780 computer, where all further processing takes place. The file transfer uses ROM-based KERMIT software.

If the set of interferogram samples started exactly at ZPD, then the source spectrum would be recovered by a pure cosine Fourier transform. As there is no means of achieving this axact start, a phase correction procedure is necessary. The procedure developed by Mertz (1967) is used.

3. Performance of the spectrometer

The spectrometer was mounted at the Cassegrain focus of the Kavalur 102 cm telescope. The interferometer and the associated electronics performed satisfactorily, apart from intermittent difficulties arising from voltage variability and interference on the mains supply. There were, however, difficulties with the fore-optics. Flexure problems arose because the counterweight limitations of the telescope (maximum permitted moment is 1800 kg × cm) did not allow a sufficiently rigid and heavy structure for the optical table. Optical astigmatism occurred because the spherical (collimator and camera) mirrors were not used in a symmetrical aberration-cancelling configuration.

Because of these limitations, it was not possible to focus stellar images on the detector element. Lunar spectra were, however, recorded successfully. A typical spectrum covering the J and H bands is shown in figure 4. It should be noted that the original spectrum contained bursts of interference, which had to be

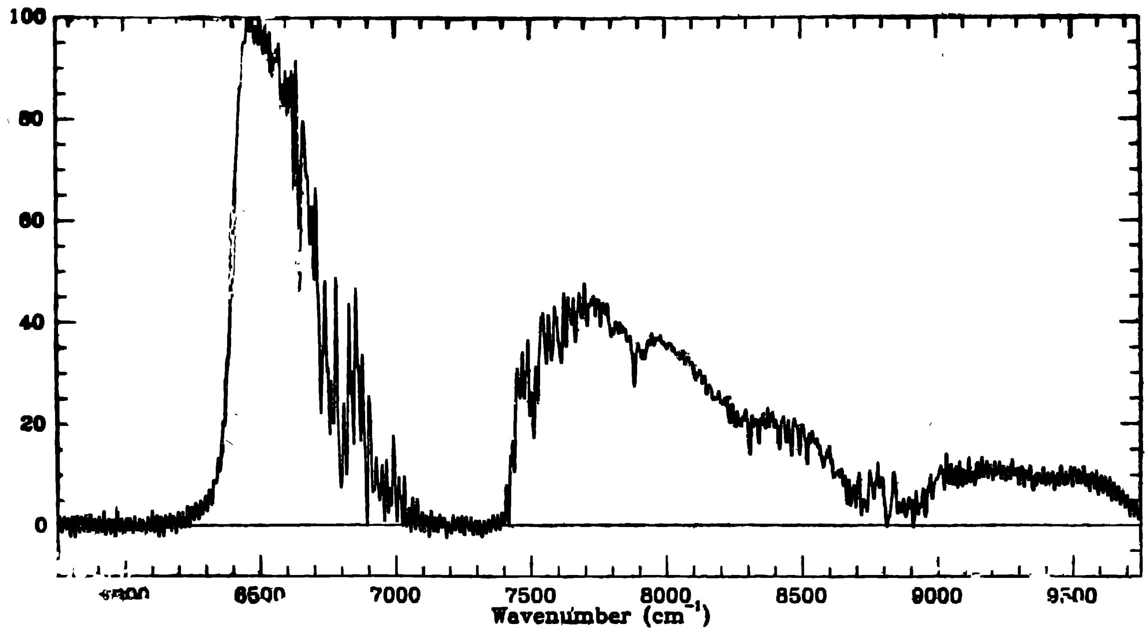

Figure 4. Lunar spectrum, in the combined J and H band, recorded with the FTS at Kavalur. The filter cut-off is shortwards of 6500 cm^{-1}.

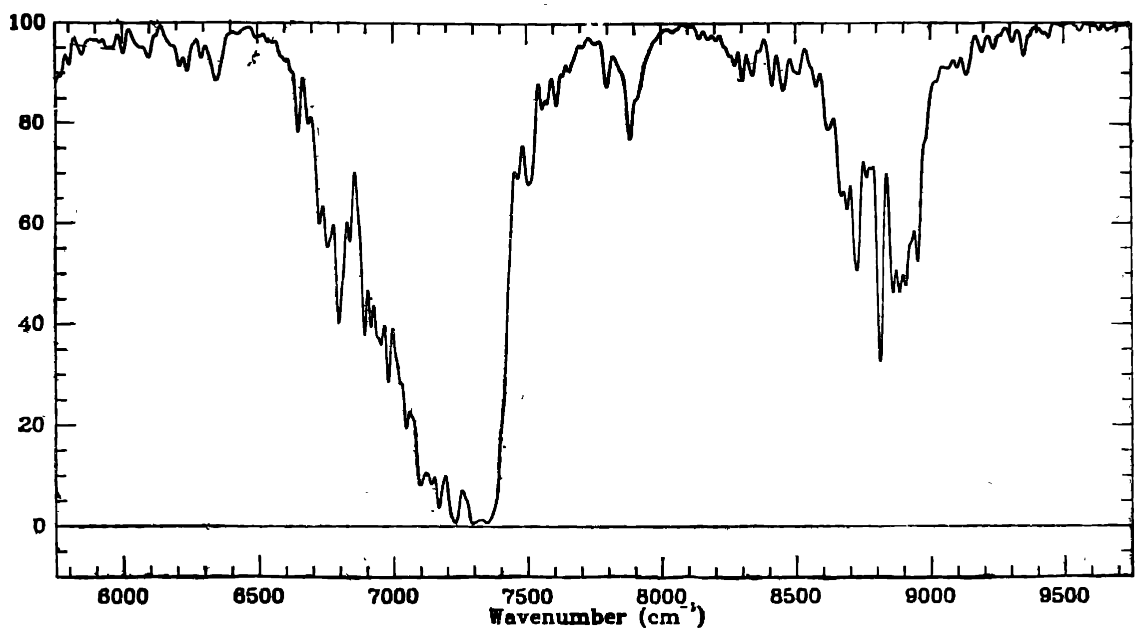

Figure 5. Solar spectrum recorded with the Mc Math FTS at Kitt Peak. The resolution has been degraded for comparison with the Kavalur lunar spectrum.

removed before transformation. There is a possibility, therefore, that the spectral structure has been somewhat distorted by this process. For comparison, the same portion of the solar spectrum published by Delbouille *et al.* (1984), degraded to the resolution of our lunar spectra, is shown in figure 5.

It is clear that the discrete features in the two spectra agree very closely. The differences between the two spectra are :

(a) The contribution from atmospheric water vapour is higher in the Kavalur spectrum because the humidity in Kavalur is much higher than at Kitt Peak. (b) The bandpass filter used at Kavalur imposes a cut-off at wavenumbers below 6500 cm^{-1}. (c) The intensity scale of the Kitt Peak spectrum has been adjusted to place the local continuum close to 100%, thus compensating for long-range variation of the sensitivity of the detection system; the Kavalur spectrum is weighted by the system response and filter characteristics. (d) The 'ripple' on the Kavalur spectrum results from missing regions of the interferogram, which were removed in the process of cleaning-up regions of the interferogram corrupted in the recording system by problems with the electrical mains.

The problems arising from the counterweight limitations of the 102 cm telescope will disappear at the Cassegrain focus of the 2.3 m telescope. A new light weight foreoptics, based on 'one-input-and-one-output' concept, is currently under fabrication for mounting the instrument at the Cassegrain of the 102 cm telescope.

Acknowledgements

We thank Prof. J. C. Bhattacharyya, Director, Indian Institute of Astrophysics, and Prof. Malcom Longair, Director, Royal Observatory, Edinburgh, for their whole-hearted support to this collaboration. S. K. J. acknowledges with thanks the help extended by the optics division of IIA, Bangalore; Mr S. C. Tapde, Mr Paul Raj, Mr Gabriel and other members of the workshop at Vainu Bappu Observatory, Kavalur.

References

Delbouille, L., *et al.* (1984) *Photometric atlas of the solar spectrum from 1,850 to 10,000 cm^{-1}*, KPNO.

Fellgett, P. B. (1951) Ph.D. thesis, University of Cambridge.

Jacquinot, P. (1954) *J. Opt. Soc. Am.* **44**, 761.

Mertz, L. (1967) *Infrared Phys.* **7**, 17.

Ridgway, S. T. & Brault, J. W. (1984) *A. Rev. Astr. Ap.* **22**, 291.

Sakai, H. (1977) in *Spectrometric techniques I* (ed. : G. A. Vanasse) Academic Press.